Pharm Res (2011) 28:776–787
DOI 10.1007/s11095-010-0330-4

RESEARCH PAPER

Actively Targeted Low-Dose Camptothecin as a Safe, Long-Acting, Disease-Modifying Nanomedicine for Rheumatoid Arthritis

Otilia May Yue Koo • Israel Rubinstein • Hayat Önyüksel

Received: 21 October 2010 / Accepted: 15 November 2010 / Published online: 4 December 2010

ABSTRACT

Purpose Camptothecin (CPT), a potent topoisomerase I inhibitor, was originally discovered as an anticancer agent to induce programmed cell death of cancer cells. Recent evidence suggests that, similar to cancer, alterations in apoptosis and over-proliferation of key effector cells in the arthritic joint result in rheumatoid arthritis (RA) pathogenesis. Initial *in vitro* studies have suggested that camptothecin inhibits synoviocyte proliferation, matrix metalloproteinases expression in chrondrocytes and angiogenesis. This study is one of the first to test, *in vivo*, RA as a new indication for CPT.

Methods To circumvent insolubility, instability and toxicity of CPT, we used biocompatible, biodegradable and targeted sterically stabilized micelles (SSM) as nanocarriers for CPT (CPT-SSM). We also surface-modified CPT-SSM with vasoactive intestinal peptide (VIP) for active targeting. We then determined whether this nanomedicine abrogated collagen-induced arthritis (CIA) in mice.

Results Based on our findings, this is the first study to report that CPT was found to be efficacious against CIA at concentrations significantly lower than usual anti-cancer dose. Furthermore, a single subcutaneous injection of CPT-SSM-VIP (0.1 mg/kg) administered to CIA mice mitigated joint inflammation for at least 32 days thereafter without systemic toxicity. CPT alone needed at least 10-fold higher dose to achieve the same effect, albeit with some vacuolization in liver histology.

Conclusion We propose that CPT-SSM-VIP is a promising targeted nanomedicine and should be further developed as a safe, long-acting, disease-modifying pharmaceutical product for RA.

KEY WORDS camptothecin · phospholipid micelles · rheumatoid arthritis · targeted drug delivery · vasoactive intestinal peptide

ABBREVIATIONS

CIA	collagen-induced arthritis
CMC	critical micelle concentration
CPT	camptothecin
CPT-SSM	sterically stabilized micelles loaded with camptothecin
CPT-SSM-VIP	sterically stabilized micelles loaded with camptothecin and surface-modified with vasoactive intestinal peptide
MTX	methotrexate

All research was conducted by author at University of Illinois at Chicago

O. M. Y. Koo • H. Önyüksel (✉)
Department of Biopharmaceutical Sciences (M/C 865)
College of Pharmacy, University of Illinois at Chicago
833 South Wood St.
Chicago, Illinois 60612-7231, USA
e-mail: hayat@uic.edu

O. M. Y. Koo
e-mail: otilia.koo@bms.com

I. Rubinstein
Department of Medicine, University of Illinois at Chicago
840 S. Wood St.
Chicago, Illinois 60612, USA
e-mail: irubinst@uic.edu

I. Rubinstein
Jesse Brown VA Medical Center
820 S. Damen Ave.
Chicago, Illinois 60612, USA

H. Önyüksel
Department of Bioengineering, University of Illinois at Chicago
851 S Morgan St.
Chicago, Illinois 60607, USA

O. M. Y. Koo
Biopharmaceutics R&D, Bristol-Myers Squibb Company
1 Squibb Dr.
New Brunswick, New Jersey 08903, USA

PEG	polyethylene glycol
RA	rheumatoid arthritis
SSM	sterically stabilized micelles
VIP	vasoactive intestinal peptide

INTRODUCTION

Rheumatoid arthritis (RA) is a chronic, debilitating autoimmune disease that afflicts ~1% of the general population (1). Despite recent advances in medical therapeutics, treatment of rheumatoid arthritis still represents an unmet medical need because of safety and efficacy concerns with currently prescribed drugs. Withdrawal of certain COX-2 inhibitors from the U.S. market due to adverse cardiovascular events illustrates this point (2). In addition, 20% to 40% of patients with RA fail to respond adequately to disease-modifying drugs (DMDs), such as methotrexate (MTX) and monoclonal anti-TNF-α antibodies (3,4). The use of DMDs is also associated with serious adverse events, such as liver injury, myelosuppression, tuberculosis, fungal infections and lymphomas (5). Increasing evidence suggests that impaired programmed cell death of inflammatory cells (T- and B-lymphocytes and macrophages), fibroblasts and synoviocytes present in the synovium of patients with RA could play a seminal role in disease pathogenesis (1). Proliferation of fibroblast-like synoviocytes adjacent to sites of joint destruction also mimics tumor cell growth (6). Recently, researchers have also begun to discover molecular pathways linking inflammation and cancer (7). In the microenvironments of tumors, key inflammatory components, such as infiltration of white blood cells, cytokines such as TNF, IL-1, IL-6 and inflammatory chemokines, can be found. Inflammatory mediators have also been implicated to cause accumulated genetic instability in cancer cells.

Camptothecin (CPT), a topoisomerase I inhibitor originally used as an anti-cancer drug, elicits programmed cell death of actively dividing cells by inhibiting topoisomerase I-DNA complex, thereby blocking further DNA synthesis and cell division leading to programmed cell death (8). Recent *in vitro* studies have found that CPT was particularly effective in inhibiting synoviocyte profliferation, angiogenesis and collagenases expression (9). Our study is one of the first to explore, in an established animal model of RA, if RA is a new indication for CPT. Unfortunately, the proposed use of CPT *in vivo* is hampered by serious formulation and delivery problems, particularly poor aqueous solubility, instability and systemic toxicity (10). Clinical application of CPT is mostly limited by its side effects, such as myelosuppression, hematological toxicity, hemorrhagic renal cystitis and elevations in liver function tests (11). Presently, there is no commercial formulation of CPT due to these delivery challenges. To overcome these problems, we developed sterically stabilized micelles (SSM) as biocompatible, biodegradable long-circulating nanocarriers (~13 nm) for CPT. We have previously reported that CPT-SSM increased drug solubility and stability by 25- and 3-fold, respectively, in comparison to CPT alone (12). Our approach to use SSM composed of PEGylated phospholipids as carriers also aims to increase CPT activity by enhancing *in vivo* stability. PEGylation of nanoparticles stabilizes them against aggregation induced by salts and proteins present in the serum (13). Given the leaky microcirculation (14) present in the inflamed interstitium of the arthritic joint and the long-circulating property of SSM (15), we reasoned that CPT-SSM should be passively targeted to the arthritic joint by selectively extravasating through leaky (pore size, ~100 nm) but not normal (pore size, <5 nm) microvascular wall. Here, we investigated if CPT in SSM nanocarriers can be targeted to the arthritic joint to show anti-arthritic efficacy at appreciably reduced doses, without hardly any systemic toxicity as CPT alone.

Overexpression of vasoactive intestinal peptide (VIP) receptors, predominantly $VPAC_2$, occurs in key effector cells, activated T-lymphocytes, macrophages and overproliferating synoviocytes (16,17). Here, we further surface-modified CPT-SSM with covalently conjugated VIP (CPT-SSM-VIP) to actively seek and bind overexpressed VIP receptors in activated T-lymphocytes and macrophages in RA site. Our innovative approach of active targeting long-circulating CPT-SSM-VIP to the effector cells in the arthritic joint should further enhance efficacy of the drug and diminish systemic toxicity.

In this study, we tested whether a single subcutaneous injection of low-dose CPT-SSM-VIP administered to mice with collagen-induced arthritis (CIA), a well-established model of RA (18), abrogated joint inflammation with no apparent systemic toxicity. Efficacy and safety of CPT-SSM-VIP were also compared to MTX and irinotecan, water-soluble CPT analog used clinically and available commercially.

METHODS

Induction, Treatment, and Assessment of CIA

In conducting research using animals, the studies were carried out in accordance to the UIC Institutional Animal Care Committee guidelines (ACC protocols #03-167 and #04-043). Male DBA/1 J mice (6–8 weeks old, 20–25 g) purchased from Jackson Laboratory (Bar Harbor, ME) were allowed to acclimatize for at least 1 week before they were injected with type II bovine collagen (CII) to induce arthritis. Native CII (Sigma Chemical Co, St. Louis, MO) was dissolved in 0.05 M acetic acid at 4°C overnight and

emulsified with an equal volume of complete Freund's adjuvant (Sigma Chemical Co, St. Louis, MO). On Day 0, mice were injected intradermally at the base of the tail with 0.15 ml of the emulsion (200 μg CII/animal). At Day 21, after primary immunization, the mice were injected intraperitoneally with a second booster dose of 200 μg CII dissolved in phosphate-buffered saline, pH 7.4. On Day 28, animals with clinical arthritic scores of ≥2 were administered treatment at respective doses. The animals were subsequently monitored until Day 60, when they were sacrificed. An exception was made for animals used for safety studies, where animals were sacrificed on Day 38 (i.e. 10 days after injection) or Day 60 to determine if they experienced any acute or delayed toxic effects, respectively.

Mice were monitored every other day for their well-being, body weights and arthritic symptoms using two parameters: paw swelling and clinical arthritis score. Paw swelling was assessed by measuring the thickness of the affected hind paws using 0–10-mm digital calipers. Clinical arthritis score was assessed by using the following system: 0, no swelling; 1, slight swelling and erythema; 2, pronounced edema; 3, joint rigidity (18). Each limb was graded, giving a maximum possible score of 12 per animal (4 paws of 3 each). Data were expressed as change in paw thickness from Day 28 values = (Paw thickness on Day X −Paw thickness on Day 28); change in clinical arthritis score from Day 28 values = (Clinical arthritis score on Day X−Clinical arthritis score on Day 28); area under the curve (AUC) = total area under the paw thickness with time curve or clinical arthritis score with time curve.

Preparation of Formulations

CPT (99% purity) was a gift from Boehringer-Ingelheim Fine Chemicals (Ingelheim, Germany). CPT-SSM was prepared by coprecipitation/reconstitution method and characterized as described previously (12). CPT alone was solubilized in a solvent buffer system (PEG_{400}:H_3PO_4 = 1:1) as used in literature (19). DSPE-PEG_{3400}-VIP conjugate was prepared by the following conditions as optimized in our laboratory (15): VIP (synthesized, using solid-phase synthesis by Dr. Bob Lee at the Protein Research Laboratory, Resources Center, UIC) and DSPE-PEG_{3400}-NHS [1,2-dioleoyl-sn-glycero-3-phosphoethanolamine-n-[poly(ethylene glycol)-M.W.=3,400]-N- succinimidyl propionate (Nektar Therapeutics Inc, Huntsville, AL) in the molar ratio of 1:5 (VIP:DSPE-PEG3400-NHS) were dissolved separately in 0.01 M isotonic HEPES buffer, pH 6.6. DSPE-PEG_{3400}-NHS was added in small increments over 1–2 min to the VIP solution at 4°C with gentle stirring. The reaction was allowed to proceed for 2 h at 4°C and then stopped by adding 1 M glycine solution (10 μl) to the reaction mixture to consume the remaining NHS moieties. CPT-SSM-VIP was formed by incubating DSPE-PEG_{3400}-VIP with CPT-SSM for at least 1 h at 25°C. Methotrexate injection USP (American Pharmaceutical Partners, Schaumburg, IL, USA) and irinotecan (Camptosar®, Pfizer Inc, NY, NY, USA) were purchased and used as supplied.

Histological and Radiographic Analyses

All the scoring in these analyses was done in a blinded fashion. Hind limbs from mice sacrificed on Day 60 were randomly collected from 5 to 6 animals and fixed with 10% buffered formalin. Subsequently, the paws were decalcified in 5% formic acid and embedded in paraffin, and 5-μm sections were stained with hematoxilin/eosin/safranin-O. Scoring was as used previously for the same animal model (20). Infiltration of cells in the joints was scored on a scale of 0–3, based on the amount of inflammatory cells in the synovial cavity (exudates) and synovial tissue (infiltrate). Cartilage destruction was graded on a scale of 0–3, ranging from the appearance of dead chondrocyte (empty lacunae) to complete loss of the articular cartilage. Bone erosions were graded on a scale of 0–3, ranging from normal bone appearance to fully eroded cortical bone structure in patella and femur condyle. The scores from the joints based on the parameters as described above were pooled, and the data were averaged per group. Four joints per hind limb from each animal were evaluated, giving a maximum score of 9/joint, 36/animal.

Hind limbs from mice sacrificed on Day 60 were randomly collected from 5 to 6 animals and fixed with 10% buffered-formalin. Radiographs of the hind limbs were taken using a General Electric (GE) mammography X-ray machine (UIC Hospital, Department of Radiology) and the following parameters: 8 mA, 24 kV, magnification factor 1.9 and a focal spot size of 0.1 mm for enhanced sensitivity and precision. Radiographs were scored in terms of a) number of joints affected and b) on a scale of 0–4, where 0—no radiographic changes, 1—equivocal findings (uncertain significance, ambiguous), 2—beginning erosions and joint space narrowing, 3—advanced erosions and joint space narrowing, 4—severe erosions and loss of joint space (21). Four joints per hind limb from each animal were evaluated, giving a maximum score of 4/joint; 16/animal.

Immunohistochemical Staining

The joint sections were deparaffinized in xylene, followed by alcohol washings. The slides were then placed in 3% hydrogen peroxide in methanol for 15 min and rinsed with Optimax wash buffer (BioGenex, San Ramon, CA) for 5 min. For CD3 and CD79 antigen unmasking, slides were microwaved in citrate buffer, pH 6. For lysozyme antigen unmasking, trypsin (0.1%) for 40 min at 37°C was used.

Avidin and biotin blocking was applied, and slides were then rinsed with buffer. Primary antibody was applied to positive slides, and buffer or negative control serum was applied to negative slides. Polyclonal rabbit anti-human/mouse CD3 (Catalog # A0452, DakoCytomation, Carpinteria, CA), monoclonal mouse anti-human CD79a, clone HM57 (Catalog # M7051, DakoCytomation, Carpinteria, CA) and rabbit anti-mouse lysozyme (Catalog # A0099, DakoCytomation, Carpinteria, CA) were incubated for 1 h (CD3 and CD79) and 30 min (lysozyme), respectively. Biotinylated secondary antibody (BioGenex Supersensitive Multilink, San Ramon, CA), labeling reagent (BioGenex Streptavidin Peroxidase, San Ramon, CA), and DAB chromogen were subsequently added to the slides before counterstaining in hematoxylin, dehydration and mounting.

Inflammatory cellular infiltration was scored as 1—minimal, 2—mild, 3—moderate, 4—marked; each of these levels was further divided into sublevels of cellular distribution ranging from 0.25—focal, 0.50—multifocal, 0.75—locally

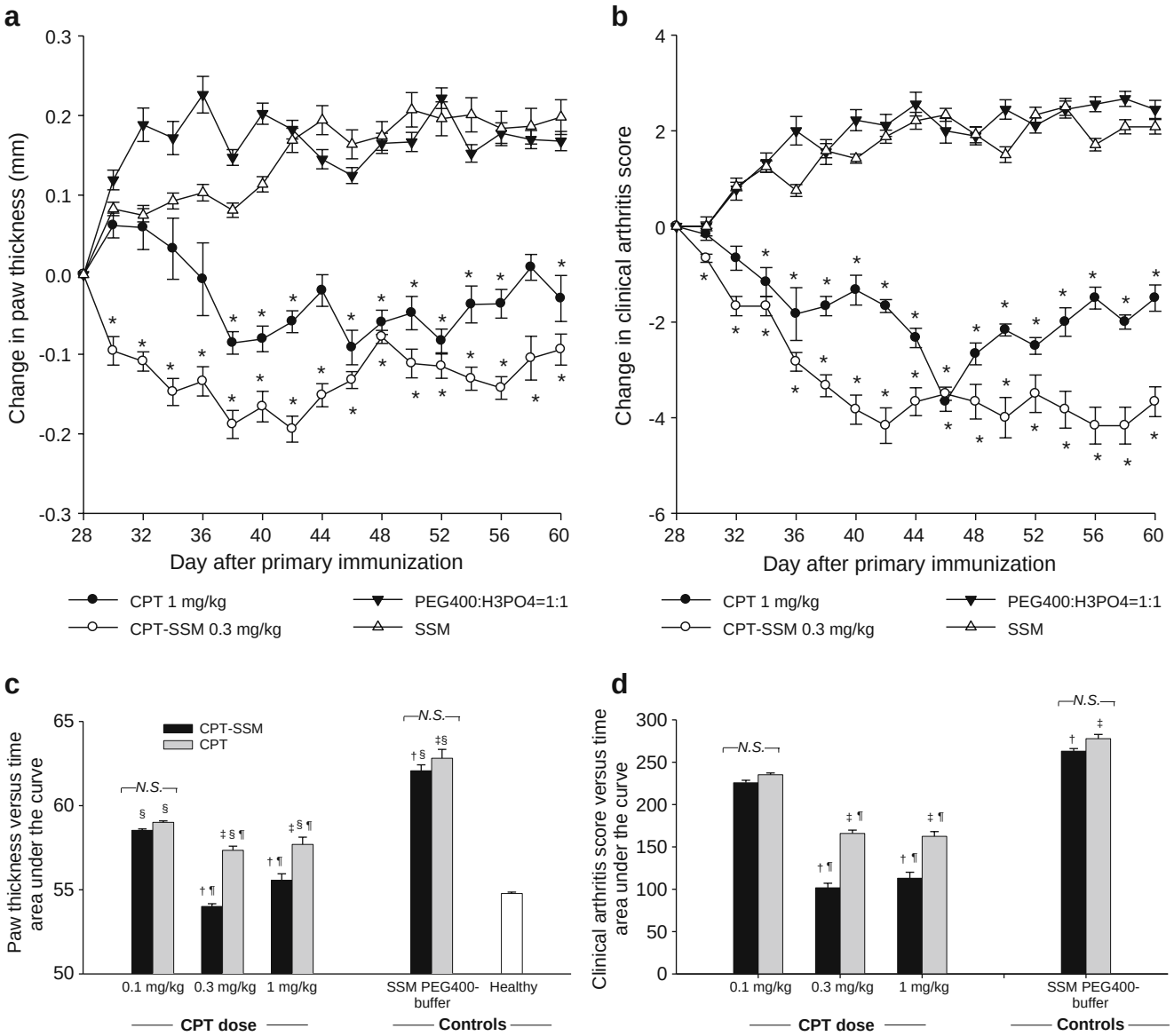

Fig. 1 CPT was effective against CIA, and efficacy was increased when CPT was delivered as CPT-SSM. Change in (**a**) paw thickness and (**b**) clinical arthritis scores of CIA mice with time. Injected with (●) 1 mg/kg CPT alone, (○) 0.3 mg/kg CPT-SSM, (▼) solvent-buffer, and (Δ) SSM. Paw thickness measurements and clinical arthritis scores were expressed as change from Day 28 values (day treatment injected). *$p < 0.05$ significant reduction *versus* Day 28 (day treatment injected). Cumulative area under the curves of (**c**) paw thickness *versus* time and (**d**) clinical arthritis score *versus* time of CIA mice treated with (▮) CPT-SSM or (□) CPT alone. Cumulative areas under the curve were calculated to indicate the relative extents of CIA symptoms. † $p < 0.05$ CPT-SSM *versus* SSM; ‡ $p < 0.05$ CPT *versus* solvent-buffer; § $p < 0.05$ *versus* normal mice; ¶ $p < 0.05$ CPT-SSM *versus* CPT alone. *N.S.* indicates not significantly different ($p > 0.05$). Results are expressed as mean ± S.E.M. (6 mice/group).

extensive. Scores from four joints (maximum score of 4/joint) of each animal were pooled, and the average pooled score from four animals per group was calculated (maximum average pooled score was 16/animal). Preparation and scoring of the slides were conducted in a blinded fashion.

Statistical Analysis

All statistical analysis was performed using the SPSS software (version 11, SPSS Inc, Chicago, IL). We analyzed changes and group differences by one-way ANOVA and then by student's *t*-test with Bonferroni correction. Area under curve (AUC) of the paw thickness–time and clinical arthritis score–time profiles were computed using SigmaPlot software (version 9, Systat Software Inc., Point Richmond, CA). All results were expressed as mean ± S.E.M. (error bars on the graphs) from at least six mice/group, except immunohitochemical study, where four mice/group. Differences were considered significant when $p<0.05$.

RESULTS

CPT Effective Against Collagen-Induced Arthritis, CPT in SSM More Efficacious than Free CPT

Mice with CIA exhibiting clinical arthritic symptoms were injected subcutaneously with increasing CPT doses (0.1–1 mg/kg) either as free CPT or CPT-SSM. Single CPT doses of 1 mg/kg as free form were effective to decrease the severity of CIA as indicated by reduction in paw swelling and clinical arthritis score from Day 28 values (day of drug injection) (Fig. 1A and B). CPT delivered at a lower dose in SSM (0.3 mg/kg) was more efficacious than free CPT at a higher dose of 1 mg/kg, as demonstrated in greater reductions in paw swelling and clinical arthritis score. Area under the curve values of paw thickness *versus* time and clinical arthritis score *versus* time were computed to further compare the relative efficacy of CPT alone and CPT-SSM at different doses (Fig. 1C and D). Smaller area under the curve values represent less severity in CIA symptoms during the study. We did not observe a dose-response relationship in the protection of CPT-SSM in CIA. There was no significant difference in area under the curve values of paw thickness *versus* time for mice injected with 0.3 mg/kg and 1 mg/kg CPT-SSM compared to normal, unimmunized DBA/1 mice (Fig. 1C). Free CPT (0.3 mg/kg and 1 mg/kg) was effective to decrease CIA compared to control PEG_{400}-buffer-injected mice with significantly smaller area under the curve values. However, these doses of free CPT did not reduce CIA to the same extent as similar doses of CPT-SSM. There was no significant difference in paw thickness and clinical arthritis score among the control groups injected with empty carriers or buffer (ANOVA, $p>0.05$) (Fig. 1C and D).

CPT-SSM-VIP Exerts Anti-arthritic Effects at Lower CPT Doses than CPT-SSM and CPT Alone

Although others have shown that VIP is effective in abolishing CIA (20), in this study, we used VIP just for targeting purposes at dose levels (up to 100-fold) lower than therapeutic doses. This was evident from Fig. 2A and B, where empty carrier controls (SSM-VIP and SSM) did not exert anti-arthritic effects. CPT-SSM-VIP (composed of 0.1 mg/kg CPT and 0.05 nmol VIP) was effective in abrogating paw swelling and restored paw thickness and

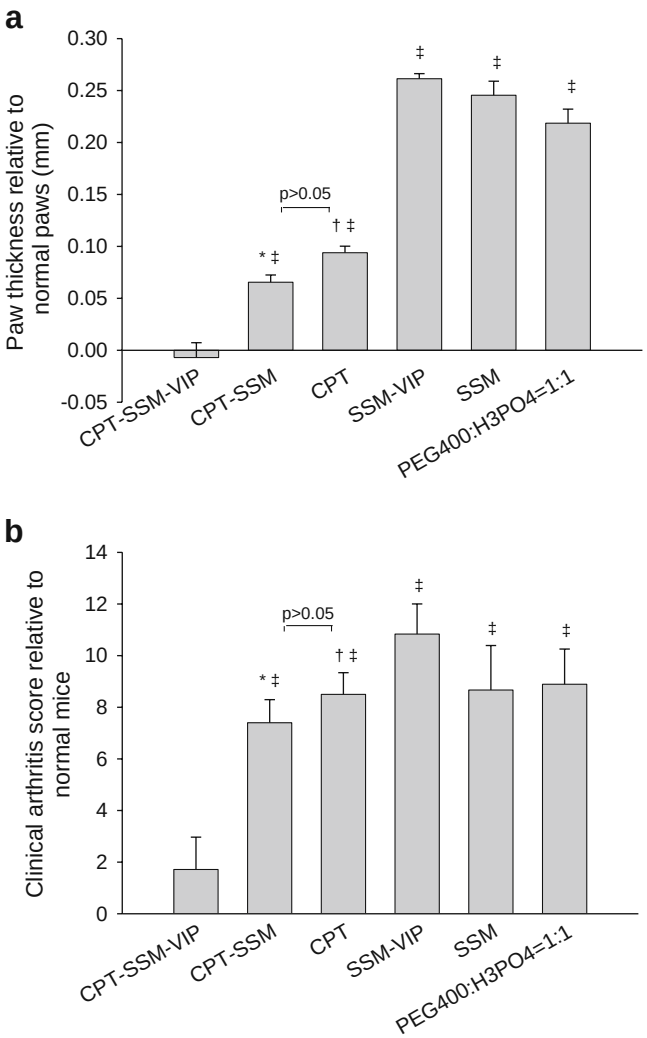

Fig. 2 CPT-SSM-VIP exerts anti-CIA action at lower CPT doses. CPT dose in all drug groups was 0.1 mg/kg. (**a**) CIA mice paws at the end of the study relative to normal unimmunized DBA/1 mice paw thickness. (**b**) Clinical arthritis scores at the end of the study relative to normal unimmunized DBA/1 mice at the end of the study. Results are expressed as mean ± S.E.M. (6 mice/group). * $p<0.05$ CPT-SSM *versus* CPT-SSM-VIP, † $p<0.05$ CPT *versus* CPT-SSM-VIP, ‡ $p<0.05$ *versus* normal mice.

clinical arthritis score similar to normal mice ($p=0.81$ *versus* normal mice) (Fig. 2A and B). We saw very little additional therapeutic effects after the first dose injections of CPT-SSM-VIP, indicating that single dose injection was sufficient to maintain protection from CIA during the remaining duration of the study. Active targeting of CPT-SSM-VIP resulted in significantly greater anti-CIA efficacy; at this low drug dose (0.1 mg/kg), CPT alone and CPT-SSM were not effective (Fig. 2A and B).

At the conclusion of the study, histopathological (Fig. 3A and B) and radiographic analyses (Fig. 3C and D) were conducted to evaluate response to the treatments, administered at their above determined preclinically effective dose levels against CIA. CPT-SSM (0.3 mg/kg CPT) and CPT-SSM-VIP (0.1 mg/kg CPT) showed complete abrogation of CIA-characteristic chronic inflammation of synovial tissues (infiltration of mononuclear cells into the joint cavity and synovial hyperplasia), pannus formation, cartilage destruction and bone erosion. Average pooled histological scores (ANOVA, $p=0.75$ and $p=0.25$ *versus* normal mice, respectively) (Fig. 3B) and average pooled radiographic scores (ANOVA, $p=0.48$ and $p=1.00$ *versus* normal mice, respectively) (Fig. 3D) of CPT-SSM-VIP (0.1 mg/kg CPT) and CPT-SSM (0.3 mg/kg CPT) were not significantly different from normal, healthy DBA/1 mice paws. CPT alone, at a 10-fold higher dose of 1 mg/kg compared to CPT-SSM-VIP, was only effective in preventing joint destruction, and radiographic scores were not significantly different from normal mice (ANOVA, $p=0.43$ *versus* normal mice) (Fig. 3D). However, with CPT alone, there was still some CIA-characteristic inflammation of the synovial tissues after CPT injection, and histological scores were not reduced back to normal levels and were still significantly different (ANOVA, $p=0.04$ *versus* normal mice) (Fig. 3B). Empty carrier control groups did not decrease the severity of CIA as observed histopathologically and radiographically.

Single Doses of MTX and Irinotecan Did Not Exert Same Anti-arthritic Effects as CPT-SSM and CPT-SSM-VIP

Methotrexate (MTX) (1 mg/kg and 10 mg/kg) and irinotecan (0.3 mg/kg) were also injected into CIA mice and monitored for paw thickness and clinical arthritis score as positive controls. Fig. 4 shows the change in paw thickness and clinical arthritis score with time after the

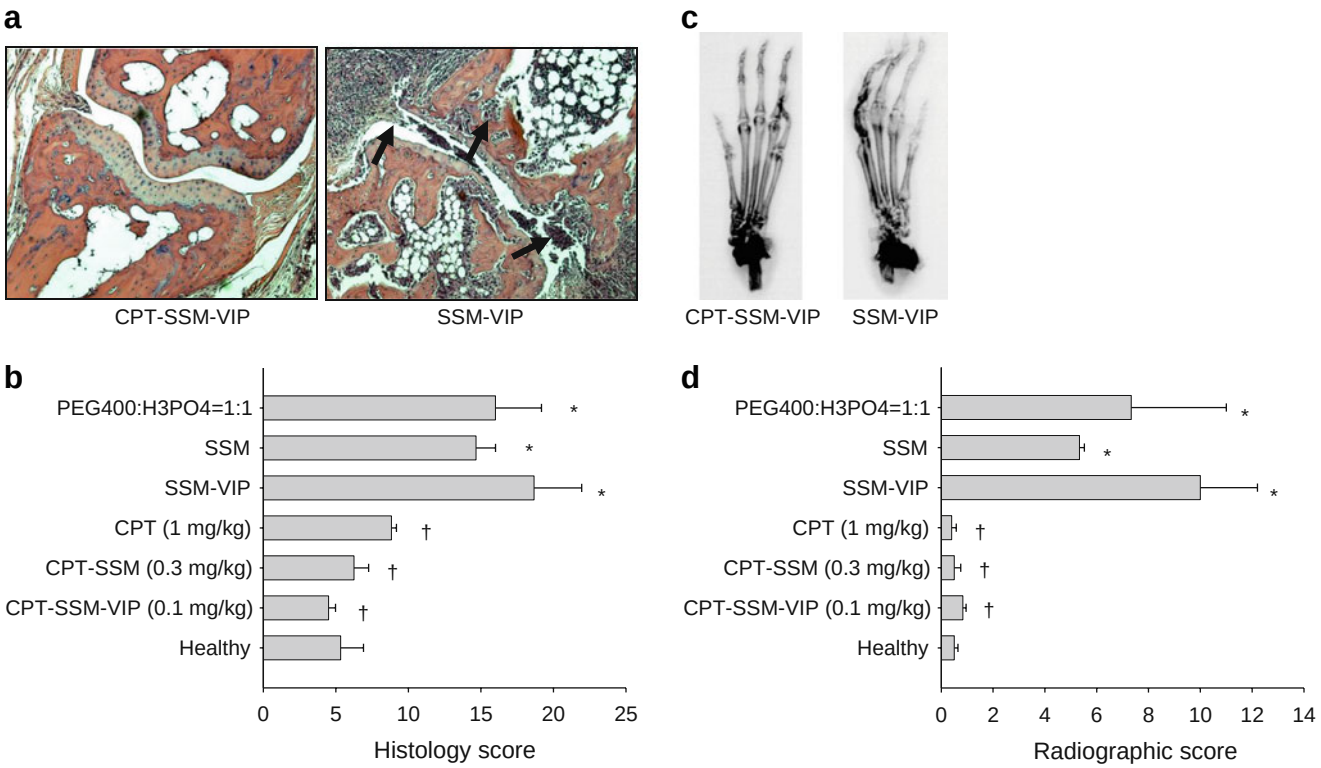

Fig. 3 CPT-SSM-VIP abrogates CIA-characteristic inflammation of the synovial tissue, cartilage destruction and bone erosion. (**a**) Representative histopathology joint section of CPT-SSM-VIP-treated (*left*) and SSM-VIP control (*right*) mice on Day 60 (magnification ×100). *Arrows* represent abnormal infiltration of inflammatory cells and bone/cartilage destruction. (**b**) Average pooled histological scores of paw sections taken from mice injected with various treatments at effective dose levels and controls. (**c**) Representative radiographs of CPT-SSM-VIP-treated (*left*) and SSM-VIP control (*right*) mice on Day 60. (**d**) Average pooled radiological scores of paw sections taken from mice injected with various treatments at effective dose levels and controls. Results are expressed as mean ± S.E.M. (6 mice/group). *$p<0.05$ *versus* normal mice, †$p<0.05$ *versus* empty controls.

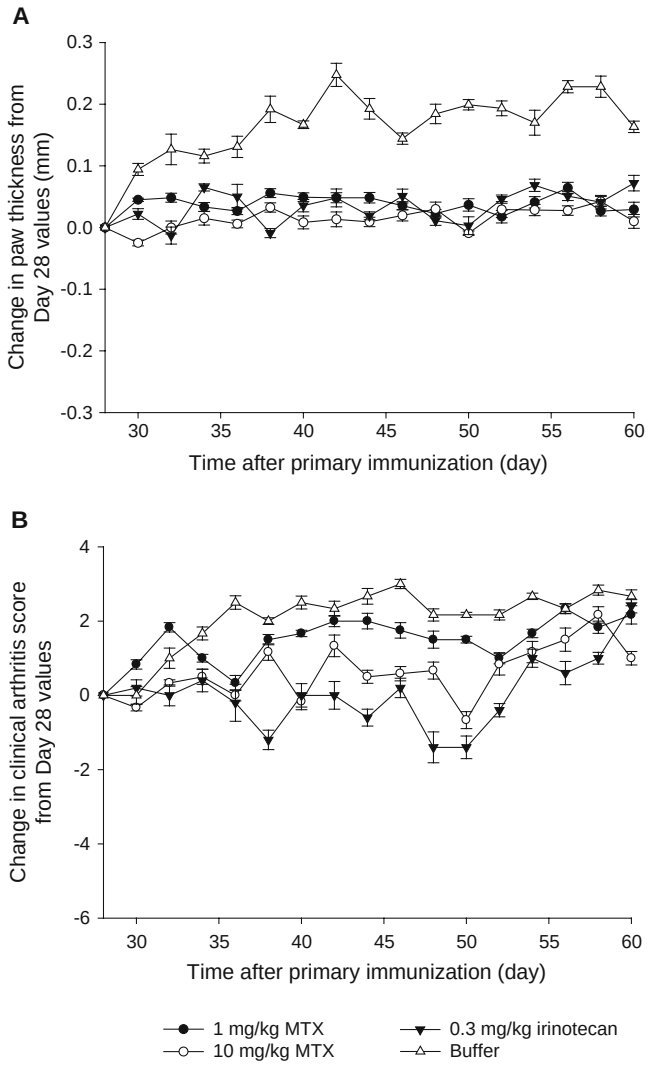

Fig. 4 Single-dose MTX and irinotecan did not result in significant reduction in CIA. Change in (**A**) paw thickness and (**B**) clinical arthritis score of CIA mice with time. Injected with (●) 1 mg/kg MTX, (○) 10 mg/kg MTX, (▼) irinotecan (0.3 mg/kg) and (Δ) solvent-buffer. Paw thickness measurements and clinical arthritis scores were expressed as change from Day 28 values (day treatment injected). Results are expressed as mean ± S.E.M. (6 mice/group).

injection. In contrast to CPT-SSM- and CPT-SSM-VIP-treated animals, mice treated with MTX and irinotecan did not exhibit a reduction of CIA symptoms back to normal values. Even though Neurath and coworkers had shown earlier that MTX was able to eliminate arthiritic conditions, they had to use 10 mg/kg every three days in CIA mice (22). In this study, a single MTX dose (1 or 10 mg/kg), similar to CPT treatment regimen, did not show abrogation of the disease. However, unlike the control buffer-treated mice, both MTX and irinotecan were effective in preventing further CIA disease progression; i.e. paw thickness and clinical arthritis scores did not worsen significantly after injection on Day 28 (ANOVA, $p>0.05$).

CPT in SSM Reduces T-Lymphocytes, Macrophage and Synoviocyte Burden in Arthritic Joint of Mice

Using immunohistochemistry, we observed that the inflammatory cells in the joints of the CIA mouse model were mostly T-lymphocytes and macrophages (Fig. 5A); B-lymphocytes were scant. This is not unexpected, since the CIA mouse model is a predominantly T-cell-driven arthritis model (23). Mice injected with empty carriers (SSM-VIP and SSM) had high cellular levels of T-lymphocytes and macrophages as well as synoviocytes proliferation in their joints. This confirms that VIP used here at up to 100-fold lower levels for targeting purposes only did not exert anti-arthritic effects. CPT delivered as CPT-SSM-VIP and CPT-SSM and injected on Day 28 caused a significant reduction in T-lymphocytes, macrophages and synoviocytes at the end of the study on Day 60 (Fig. 5B). CPT-SSM-VIP resulted in a significantly faster rate of reduction of cells compared to CPT-SSM. By Day 38 (10 days after CPT-SSM-VIP injection), the mice joints already showed significantly lower T-lymphocyte and macrophage levels than mice injected with empty carriers (Fig. 5C). CPT-SSM caused a more delayed reduction in T-lymphocytes, macrophages and synoviocytes; a significant reduction in these cells was only observed at the end of the study (Day 60 i.e. 32 days after CPT-SSM injection) (student's *t*-test, $p=0.03$ CPT-SSM *versus* SSM). On the other hand, joints from mice with CIA injected with empty SSM-VIP and SSM showed a progressive, albeit not significant, increase in the levels and distribution of T-lymphocytes, macrophages and synoviocytes from Day 38 to Day 60.

CPT in SSM Has No Deleterious Effects on Blood Parameters and Normal Tissues in Mice with CIA

Mice with CIA exhibited normal behavior, fur coat and body weight gain in all study groups. Administration of free CPT, CPT-SSM-VIP and CPT-SSM had no significant effects on blood hemoglobin and white blood cell and platelet counts (each group, $n=6$ animals; $p>0.05$ *versus* normal reference values; Table I) (24,25).

Serum ALT and AST levels at the end of the study on Day 60 were elevated in mice with CIA injected with empty SSM (Table I). Serum levels of ALT and AST were within the normative range in mice with CIA treated with free CPT, CPT-SSM-VIP or CPT-SSM (Table I). Serum creatinine and blood urea nitrogen levels were within the normative range for all CPT-treated mice with CIA (each group, $n=6$ animals; Table I). Histology of heart, lungs, kidney and spleen were normal in all the groups (each group, $n=6$ animals) (representative sections are shown in Fig. 6). As shown in Fig. 6F, some vacuolization was observed only in the H&E sections of liver tissues from mice injected with free CPT.

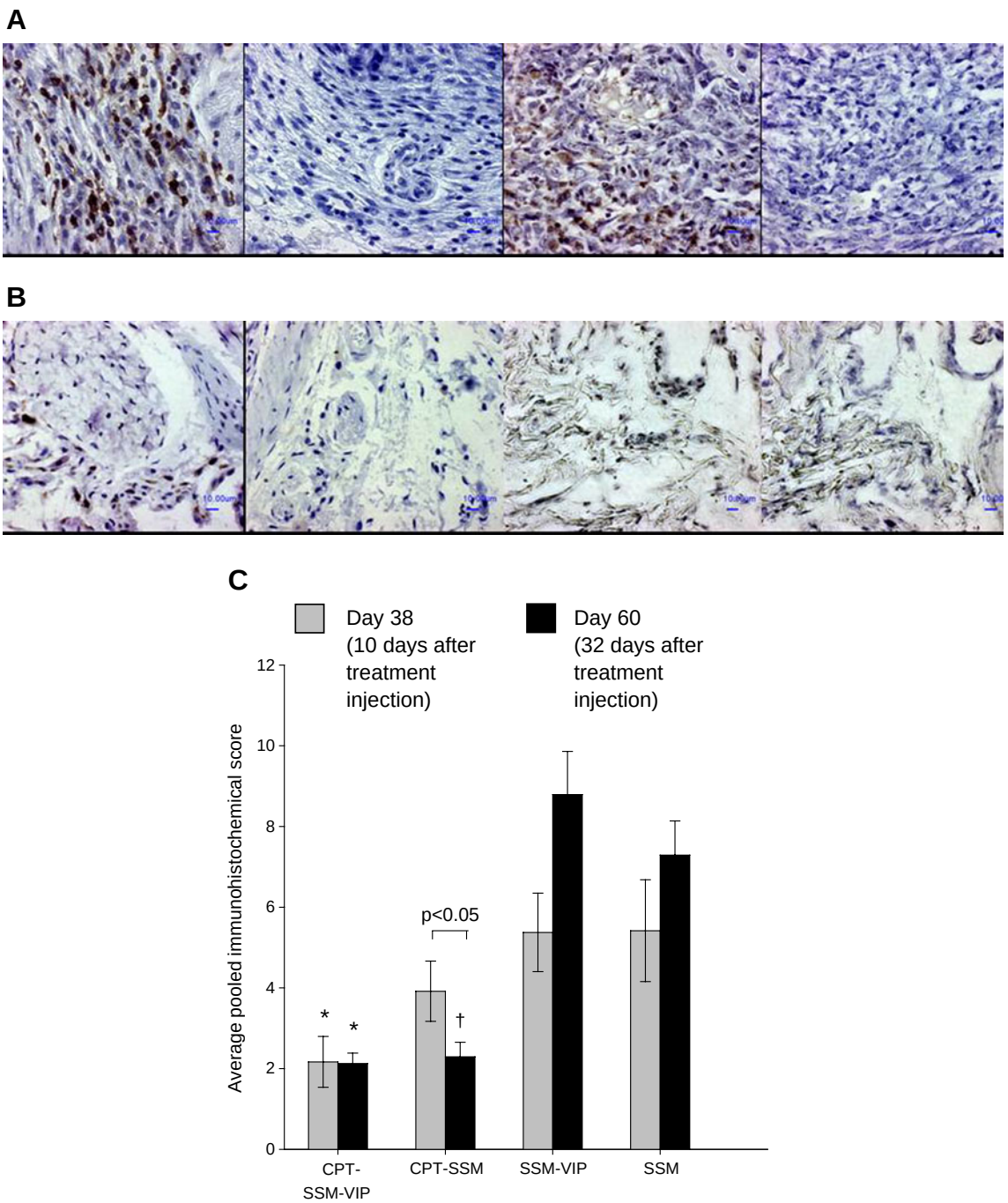

Fig. 5 CPT in micelles reduces cellular content within the CIA joints. Representative joint sections of (**A**) empty SSM-VIP-injected mice, (**B**) CPT-SSM-VIP-treated mice; (*left to right*) CD3+, CD3-, lysozyme+, lysozyme− staining. *Bars* represent 10 μm. (**C**) Average pooled immunohistochemical scores of cellular infiltration and distribution in joints of CIA mice on (□) Day 38 and (▮) Day 60. Results are expressed as mean ± S.E.M. (6 mice/group). *, † $p < 0.05$ *versus* SSM-VIP and SSM, respectively.

DISCUSSION

The results of this study showed that a single, subcutaneous injection of low-dose CPT administered in biocompatible, biodegradable, targeted phospholipid-based nanocarriers (CPT-SSM-VIP) mitigated joint inflammation for at least 32 days thereafter without systemic toxicity in CIA mice. CPT dose injected here was about 100-fold lower than that used in cancer (19). Therefore, CPT-SSM-VIP appears to be a promising nanomedicine of the future to treat RA.

A major challenge we addressed in this study was the lack of a stable, active and non-toxic formulation of CPT. Currently, there is no commercial formulation of CPT. To address this issue, we devised an innovative, safe, targeted

Table I Hematological and Serum Chemistry Parameters (CPT Dose was 0.3 mg/kg for all CPT Groups)

Parameter[a,b]	Normal	CPT-SSM-VIP	CPT-SSM	CPT alone	SSM-VIP	SSM	PEG_{400}: H_3PO_4 = 1:1
White blood cells ($\times 10^3/\mu L$)	6.8 (1.9)	5.9 (1.3)	5.6 (1.2)	8.4 (2.0)	6.5 (1.7)	7.1 (1.3)	7.9 (1.2)
Red blood cells ($\times 10^6/\mu L$)	9.1 (1.5)	9.3 (0.7)	9.7 (0.7)	10.1 (0.7)	9.3 (0.3)	10.0 (0.8)	9.8 (0.1)
Hemoglobin (g/dL)	12.7 (2.4)	12.5 (0.8)	13.0 (0.7)	13.4 (1.1)	12.3 (0.3)	13.4 (0.8)	13.1(0.4)
Hematocrit (%)	41.0 (8.1)	42.8 (2.8)	43.7 (1.5)	45.4 (3.0)	41.0 (0.8)	45.8 (2.8)	44.3 (0.7)
Mean cell hemoglobin concentration (g/dL)	30.9 (0.6)	29 (0.5)	29.7 (0.5)	29.5 (0.8)	30.1 (0.2)	29.3 (0.9)	29.5 (0.6)
Platelets ($\times 10^3/\mu L$)	747 (294)	1045 (234)	1042 (158)	994 (320)	1021 (160)	998 (164)	1074 (182)
ALP (U/L)	79 (9)	84.2 (13.1)	93.8 (7.8)	84.2 (9.4)	79.7 (22.2)	97.8 (13.0)[c]	83.0 (12.5)
ALT (U/L)	38 (6.3)	30.0 (7.7)	32.3 (5.1)	39.4 (3.9)	72.4 (13.8)[c]	75.5 (15.3)[c]	51.7 (9.9)[c]
AST (U/L)	82 (45)	95.8 (8.3)	107.8 (8.2)	105.4 (8.5)	155.7 (22.7)[c]	201.3 (48.2)[c]	132.3 (23.2)[c]
Na (mmol/l)	158 (8.6)	150.6 (1.1)	149.8 (2.7)	150.1 (1.8)	145.8 (6.0)	147.2 (4.7)	150.3 (3.4)
K (mmol/l)	8.3 (1.3)	4.4 (0.4)	4.1 (0.3)	4.7 (0.8)	4.2 (0.7)	4.5 (0.9)	4.2 (0.5)
Cl (mmol/l)	120 (5.6)	112.5 (1.4)	110.4 (4.1)	111.4 (0.7)	107.8 (5.7)	108.9 (3.9)	112.5 (1.2)
Creatinine (μmol/l)[d]	1.0 (2.2)	N.D.	N.D.	N.D.	N.D.	N.D.	N.D.
Blood urea nitrogen	34.0 (9.7)	23.5 (10.2)	27.5 (3.3)	24.4 (3.3)	23.8 (2.4)	23.1 (6.5)	22.0 (2.2)
Total protein (g/dl)	5.2 (0.6)	4.3 (0.4)	4.4 (0.2)	4.4 (0.1)	4.1 (0.8)	4.3 (0.4)	4.2 (0.1)
Albumin (g/dl)	3.0 (0.3)	2.9 (0.2)	2.8 (0.1)	2.7 (0.2)	2.5 (0.6)	2.7 (0.2)	2.6 (0.1)
Globulin (g/dl)	1.3 (0.2)	1.4 (0.3)	1.5 (0.3)	1.7 (0.1)	1.6 (0.4)	1.6 (0.2)	1.6 (0.0)

[a] Normal values for hematological parameters were measured using unimmunized mice and serum chemistry values were taken from Refs (19) and (20).

[b] Values are means of $n = 6$/group, S.D. are in brackets.

[c] Indicates significantly different from normal range.

[d] Serum creatinine is below detection (*N.D.*)

nanocarrier system, sterically stabilized micelles for CPT delivery (CPT-SSM). We found that this construct resulted in a 3-fold improvement in arthritis in mice with CIA relative to CPT alone and for a longer period of time. There are multiple plausible explanations for the beneficial effects of CPT-SSM over free CPT in this model. First, SSM, composed of biocompatible PEGylated phospholipid molecules, improved solubilization and stabilization of CPT in aqueous solution (12). Previously, we have found that the critical micelle concentration (CMC) of SSM was in the micromolar range (0.5–1.5 μM) (26); thus, SSMs are thermodynamically more stable upon *in vivo* dilution than conventional detergent micelles, which usually have CMCs in millimolar ranges. Within the hydrophobic core of phospholipid micelles, similar to liposomes (27), hydrolytic transformation of CPT lactone to inactive carboxylate was reduced, resulting in more active CPT in a given dose to evoke programmed cell death of key effector cells in the arthritic joint.

CPT-SSM, which is ~13 nm in size (12,26), extravasates selectively through the leaky microcirculation (post-capillary venules) of the inflamed arthritic joint. However, this nanomedicine is too large to extravasate through the intact microvascular wall of healthy tissues, such as kidney and bone marrow. Moreover, PEG_{2000} grafted to phospholipid molecules confers steric hindrance to the nanomedicine, thereby preventing its opsonization in the serum and uptake by the liver and other tissues of the reticuloendothelial system (28). We have shown in this study that both of these phenomena improved bioavailability of CPT-SSM because of prolonged circulation time and preferential extravasation into the arthritic joints. The latter reduced the effective dose and drug toxicity to susceptible normal tissues, such as liver, bone marrow and kidney, thereby improving the therapeutic index of CPT-SSM.

Currently, there is no commercial product of CPT in the market; however, CPT has been formulated and delivered as liposome-encapsulated (27,29) and PEG-grafted forms (30). Clinical trials with PEG-camptothecin, which involves the chemical modification of the drug molecule, have yet to demonstrate its activity against various cancers (31). Preparation and storage of liposomal CPT products are more complicated than CPT-SSM developed in this study. We have already shown that VIP-targeted micellar CPT can be prepared and stored in a lyophilized form and reconstituted to obtain original properties before use (12). Furthermore, the passive targeting of SSM should be more efficient due to its smaller size compared to liposomes. SSM itself is composed of biocompatible phospholipids as excipient in an already US FDA approved marketed formulation

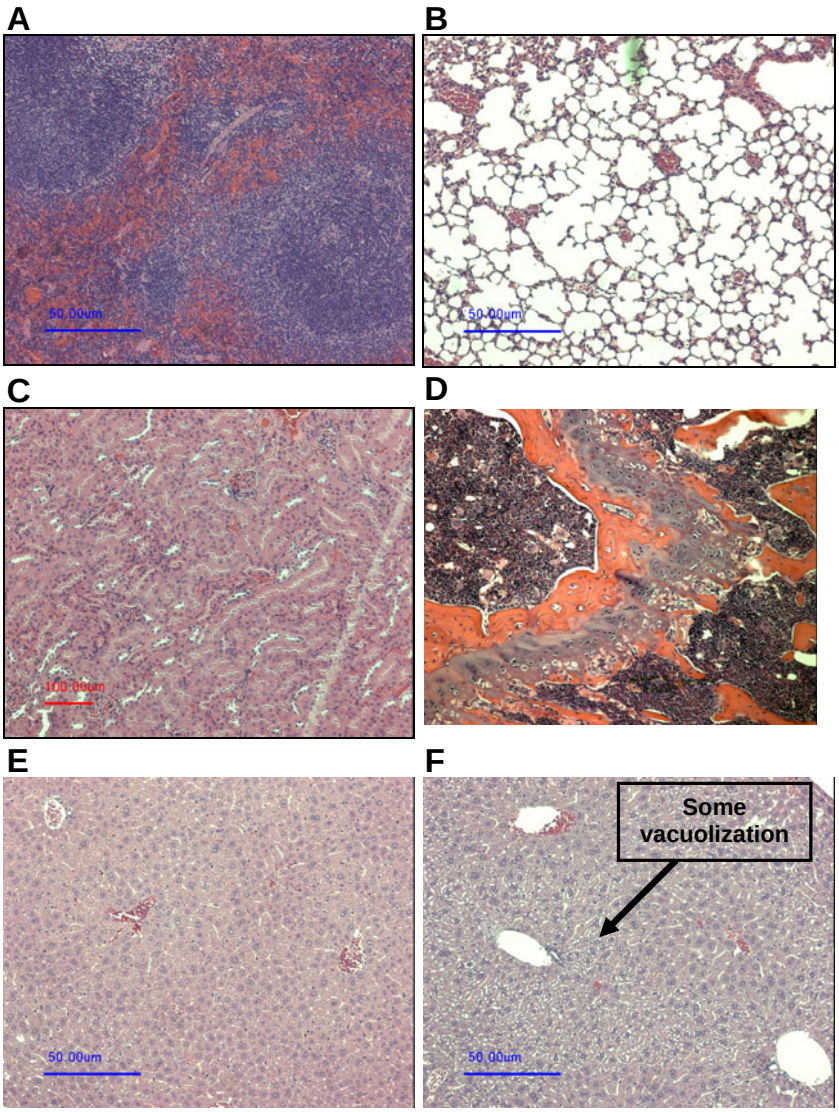

Fig. 6 Representative H&E sections of major organs. (**A**) spleen, (**B**) lung, (**C**) kidney, (**D**) bone marrow, (**E**) liver from mice injected with CPT-SSM; (**F**) liver from mice injected with free CPT. *Bar* represents 50 μm.

Doxil®; thus, it is safe as nanocarrier when administered in animals and humans (32). We have also tested irinotecan, a CPT analog used clinically and have found that comparable doses of irinotecan administered as a single dose did not significantly reduce CIA, albeit the progression of CIA was prevented. Irinotecan, being water soluble and molecularly dispersed in the blood, is not passively targeted to inflamed sites due to being able to extravase out of the circulation. Therefore, higher doses, with possible side effects, are needed to achieve the same effect as targeted nanomedicine formulation of CPT developed in this study. Similarly, we have observed that single dose of CPT-SSM and CPT-SSM-VIP reduced CIA symptoms significantly, whilst MTX did not.

Although recent *in vitro* studies have found that CPT, a topoisomerase I inhibitor, was particularly effective in inhibiting synoviocyte profliferation, angiogenesis and collagenases expression for arthritis (9), our study is one of the first to show the anti-arthritic effects of CPT *in vivo* in CIA mice. The longer-lasting anti-arthritic effects of CPT over MTX suggest potential advantages of topoisomerase I inhibition; additional mechanistic studies are warranted to further understand this.

$VPAC_2$ receptors are induced in activated T-lymphocytes, macrophages and over-proliferating synoviocytes in the arthritic joint (16,20,33). Therefore, we exploited this phenomenon to actively target CPT-SSM to arthritic joints of mice with CIA using VIP as the targeting ligand. This approach further amplified the salutary effects of CPT-SSM-VIP in the arthritic joint relative to CPT alone and CPT-SSM at a substantially lower dose (Fig. 2A and B). We have previously used this approach to target technetium-loaded sterically stabilized liposomes with VIP to *in situ* breast cancer in rats (15). The use of VIP as a ligand for active targeting of CPT-SSM in mice with CIA has several distinct attributes over existing ligands, such as

monoclonal antibodies and folate (34,35). First, VIP, a 28-amino acid mammalian peptide, is an endogenous peptide and, hence, non-immunogenic. It can be synthesized in large quantities. In addition, we have previously shown that association of VIP with SSM leads to conformational transition of the peptide molecule from random coil in aqueous solution to α-helix in lipids (36,37). The latter is the optimal conformation for ligand-receptor interactions and protects the peptide from hydrolysis, degradation and inactivation *in vivo*. Importantly, VIP receptors are expressed predominantly on the abluminal (vascular smooth muscle cells) side of the normal microcirculation (38). Unlike most target receptors that exist in circulation, this phenomenon will mitigate circulating CPT-SSM-VIP interactions with lining endothelial cells, thereby prolonging its circulation time, amplifying its bioavailability and decreasing the drug toxicity to non-arthritic sites. CPT-SSM-VIP can only extravasate at the arthritic joints where the endothelial lining is disrupted (38). We have previously demonstrated that VIP-R can internalize micelles to directly deliver the micelle load into cells (39). The results of this study also suggest that once in the arthritic joint interstitium, VIP-grafted CPT-SSMs home VIP receptors over-expressed in activated T-lymphocytes, macrophages and over-proliferating synoviocytes, leading to reduced burden of activated T-lymphocytes, macrophages and over-proliferating synovocytes in the joints of mice with CIA. Further studies are indicated to elucidate the molecular mechanism(s) underlying this phenomenon. Conceivably, actively targeted CPT-SSM-VIP could induce programmed cell death of these activated cells by inhibiting topoisomerase I-DNA complex (40). This process should not affect resting cells (41), thereby accounting, in part, for the higher efficacy of low-dose actively targeted CPT-SSM-VIP in the arthritic joint.

There was no observable histological damage to major organs in mice treated with CPT-SSM-VIP and CPT-SSM, which corroborates with the normal blood cell counts and serum chemistries. CPT-SSM-VIP and CPT-SSM were safe after administration and did not cause injury to these organs.

CONCLUSION

In conclusion, we found that a single, subcutaneous injection of low-dose CPT in biocompatible, biodegradable, targeted phospholipid-based nanocarriers (CPT-SSM-VIP) administered after induction of collagen-induced arthritis in mice mitigated joint inflammation for a prolonged period thereafter without systemic toxicity. We propose that CPT-SSM-VIP should be further evaluated as a safe, long-acting disease-modifying nanomedicine for rheumatoid arthritis. Given the molecular pathways linking inflammation and cancer, we suggest that CPT-SSM-VIP used at 100-fold lower anti-inflammatory dose than anti-cancer doses can be additionally explored as a cancer preventive agent.

ACKNOWLEDGMENTS

We thank J. Artwohl for his advice on the CIA mouse model and for analyzing our histology and radiographic slides in a blinded fashion, T. Valli and the veterinarian pathology laboratory at University of Illinois at Urbana Champion for preparing the immunohistochemical slides and analyzing them in a blinded fashion, R. Gemeinhart's laboratory for use of microscope equipment, H. Radloff at the Radiology Department at UIC Hospital for help in taking the radiographs. This study was supported, in part, by DOD grant BCRP, #DAMD 17-02-1-0415, VA Merit Review and NIH grants R01 AG024026, R01 HL72323 and C06RR15482. This investigation was conducted in a facility constructed with support from grant C06RR15482 from the NIH National Center for Research Resources. O. M.K. was a recipient of the UIC University Fellowship.

REFERENCES

1. Firestein GS. Evolving concepts of rheumatoid arthritis. Nature. 2003;423:356–61.
2. Editorial: Painful lessons. Nat Struct Mol Biol. 2005;12:205.
3. Borchers AT, Keen CL, Cheema GS, Gershwin ME. The use of methotrexate in rheumatoid arthritis. Semin Arthritis Rheum. 2004;34:465–83.
4. Rubbert-Roth A, Finckh A. Treatment options in patients with rheumatoid arthritis failing initial TNF inhibitor therapy: a critical review. Arthritis Res & Therapy. 2009;11:S1.
5. O'Dell JR. Therapeutic strategies for rheumatoid arthritis. N Engl J Med. 2004;350:2591–602.
6. Liu H, Pope RM. Apoptosis in rheumatoid arthritis: friend or foe. Rheum Dis Clin North Am. 2004;30:603–25. x.
7. Colotta F, Allavena P, Sica A, Garlanda C, Mantovani A. Cancer-related inflammation, the seventh hallmark of cancer: links to genetic instability. Carcinogenesis. 2009;30:1073.
8. Stewart L, Redinbo MR, Qiu X, Hol WG, Champoux JJ. A model for the mechanism of human topoisomerase I. Science. 1998;279:1534–41.
9. Jackson JK, Higo T, Hunter WL, Burt HM. Topoisomerase inhibitors as anti-arthritic agents. Inflamm Res. 2008;57:126–34.
10. Schaeppi U, Fleischman RW, Cooney DA. Toxicity of camptothecin (NSC-100880). Cancer Chemother Rep. 3 1974;5:25–36.
11. Moertel CG, Schutt AJ, Reitemeier RJ, Hahn RG. Phase II study of camptothecin (NSC-100880) in the treatment of advanced gastrointestinal cancer. Cancer Chemother Rep. 1972;56:95–101.
12. Koo O, Rubinstein I, Onyuksel H. Camptothecin in sterically stabilized phospholipid micelles: a novel nanomedicine. Nanomedicine. 2005;1:77–84.
13. Taratula O *et al.* Surface-engineered targeted PPI dendrimer for efficient intracellular and intratumoral siRNA delivery. J Control Release. 2009;140:284–93.

14. Lu J, Kasama T, Kobayashi K, Yoda Y, Shiozawa F, Hanyuda M, *et al.* Vascular endothelial growth factor expression and regulation of murine collagen-induced arthritis. J Immunol. 2000;164:5922–7.
15. Dagar S, Krishnadas A, Rubinstein I, Blend MJ, Onyuksel H. VIP grafted sterically stabilized liposomes for targeted imaging of breast cancer: *in vivo* studies. J Control Release. 2003;91:123–33.
16. Delgado M, Pozo D, Ganea D. The significance of vasoactive intestinal Peptide in immunomodulation. Pharmacol Rev. 2004;56:249–90.
17. Delgado M, Abad C, Martinez C, Juarranz MG, Arranz A, Gomariz RP, *et al.* Vasoactive intestinal peptide in the immune system: potential therapeutic role in inflammatory and autoimmune diseases. J Mol Med. 2002;80:16–24.
18. Courtenay JS, Dallman MJ, Dayan AD, Martin A, Mosedale B. Immunisation against heterologous type II collagen induces arthritis in mice. Nature. 1980;283:666–8.
19. Caiolfa VR *et al.* Polymer-bound camptothecin: initial biodistribution and antitumour activity studies. J Control Release. 2000;65:105–19.
20. Delgado M *et al.* Genetic association of vasoactive intestinal peptide receptor with rheumatoid arthritis: altered expression and signal in immune cells. Arthritis Rheum. 2008;58:1010–9.
21. Reiff A, Zastrow M, Sun BC, Takei S, Mitsuhada H, Bernstein B, *et al.* Treatment of collagen induced arthritis in DBA/1 mice with L-asparaginase. Clin Exp Rheumatol. 2001;19:639–46.
22. Neurath MF *et al.* Methotrexate specifically modulates cytokine production by T cells and macrophages in murine collagen-induced arthritis (CIA): a mechanism for methotrexate-mediated immunosuppression. Clin Exp Immunol. 1999;115:42–55.
23. Holmdahl R, Bockermann R, Backlund J, Yamada H. The molecular pathogenesis of collagen-induced arthritis in mice—a model for rheumatoid arthritis. Ageing Res Rev. 2002;1:135–47.
24. Wolford ST *et al.* Reference range data base for serum chemistry and hematology values in laboratory animals. J Toxicol Environ Health. 1986;18:161–88.
25. Schnell MA, Hardy C, Hawley M, Propert KJ, Wilson JM. Effect of blood collection technique in mice on clinical pathology parameters. Hum Gene Ther. 2002;13:155–61.
26. Ashok B, Arleth L, Hjelm RP, Rubinstein I, Onyuksel H. *In vitro* characterization of pegylated phospholipid micelles for improved drug solubilization: effects of peg chain length and PC incorporation. J Pharm Sci. 2004;93:2476–87.
27. Burke TG, Staubus AE, Mishra AK. Liposomal stabilization of camptothecin's lactone ring. Journal of American Chemical Society. 1992;114:8318–9.
28. Koo OM, Rubinstein I, Onyuksel H. Role of nanotechnology in targeted drug delivery and imaging: a concise review. Nanomedicine. 2005;1:193–212.
29. Daoud SS, Fetouh MI, Giovanella BC. Antitumor effect of liposome-incorporated camptothecin in human malignant xenografts. Anticancer Drugs. 1995;6:83–93.
30. Rowinsky EK *et al.* A phase I and pharmacokinetic study of pegylated camptothecin as a 1-hour infusion every 3 weeks in patients with advanced solid malignancies. J Clin Oncol. 2003;21:148–57.
31. Scott LC *et al.* A phase II study of pegylated-camptothecin (pegamotecan) in the treatment of locally advanced and metastatic gastric and gastro-oesophageal junction adenocarcinoma. Cancer Chemother Pharmacol. 2009;63:363–70.
32. Working PK, Dayan AD. Pharmacological-toxicological expert report. CAELYX. (Stealth liposomal doxorubicin HCl). Hum Exp Toxicol. 1996;15:751–85.
33. Delgado M, Ganea D. Vasoactive intestinal peptide and pituitary adenylate cyclase-activating polypeptide inhibit nuclear factor-kappa B-dependent gene activation at multiple levels in the human monocytic cell line THP-1. J Biol Chem. 2001;276:369–80.
34. Turk MJ *et al.* Folate-targeted imaging of activated macrophages in rats with adjuvant-induced arthritis. Arthritis Rheum. 2002;46:1947–55.
35. Nagayoshi R *et al.* Effectiveness of anti-folate receptor beta antibody conjugated with truncated Pseudomonas exotoxin in the targeting of rheumatoid arthritis synovial macrophages. Arthritis Rheum. 2005;52:2666–75.
36. Rubinstein I, Patel M, Ikezaki H, Dagar S, Onyuksel H. Conformation and vasoreactivity of VIP in phospholipids: effects of calmodulin. Peptides. 1999;20:1497–501.
37. Onyuksel H, Ikezaki H, Patel M, Gao XP, Rubinstein I. A novel formulation of VIP in sterically stabilized micelles amplifies vasodilation *in vivo*. Pharm Res. 1999;16:155–60.
38. Fahrenkrug J, Hannibal J, Tams J, Georg B. Immunohistochemical localization of the VIP1 receptor (VPAC1R) in rat cerebral blood vessels: relation to PACAP and VIP containing nerves. J Cereb Blood Flow Metab. 2000;20:1205–14.
39. Rubinstein I, Soos I, Onyuksel H. Intracellular delivery of VIP-grafted sterically stabilized phospholipid mixed nanomicelles in human breast cancer cells. Chem Biol Interact. 2007;171:190–4.
40. Redinbo MR, Stewart L, Kuhn P, Champoux JJ, Hol WG. Crystal structures of human topoisomerase I in covalent and noncovalent complexes with DNA. Science. 1998;279:1504–13.
41. Ferraro C, Quemeneur L, Fournel S, Prigent AF, Revillard JP, Bonnefoy-Berard N. The topoisomerase inhibitors camptothecin and etoposide induce a CD95-independent apoptosis of activated peripheral lymphocytes. Cell Death Differ. 2000;7:197–206.